

Research Paper

Activation of cannabinoid CB1 receptors modulates evoked action potentials in rat retinal ganglion cells

JIANG Shu-Xia, LI Qian, WANG Xiao-Han, LI Fang, WANG Zhong-Feng*

Institutes of Brain Science, Institute of Neurobiology and State Key Laboratory of Medical Neurobiology, Fudan University, Shanghai 200032, China

Abstract: Activation of cannabinoid CB1 receptors (CB1Rs) regulates a variety of physiological functions in the vertebrate retina through modulating various types of ion channels. The aim of the present study was to investigate the effects of this receptor on cell excitability of rat retinal ganglion cells (RGCs) in retinal slices using whole-cell patch-clamp techniques. The results showed that under current-clamped condition perfusing WIN55212-2 (WIN, 5 $\mu\text{mol/L}$), a CB1R agonist, did not significantly change the spontaneous firing frequency and resting membrane potential of RGCs. In the presence of cocktail synaptic blockers, including excitatory postsynaptic receptor blockers CNQX and D-APV, and inhibitory receptor blockers bicuculline and strychnine, perfusion of WIN (5 $\mu\text{mol/L}$) hardly changed the frequencies of evoked action potentials by a series of positive current injection (from +10 to +100 pA). Phase-plane plot analysis showed that both average threshold voltage for triggering action potential and delay time to reach threshold voltage were not affected by WIN. However, WIN significantly decreased $+dV/dt_{\text{max}}$ and $-dV/dt_{\text{max}}$ of action potentials, suggestive of reduced rising and descending velocities of action potentials. The effects of WIN were reversed by co-application of SR141716, a CB1R selective antagonist. Moreover, WIN did not influence resting membrane potential of RGCs with synaptic inputs being blocked. These results suggest that activation of CB1Rs may regulate intrinsic excitability of rat RGCs through modulating evoked action potentials.

Key words: action potential; cannabinoid CB1 receptor; patch-clamp; retinal ganglion cell; spontaneous firing; WIN55212-2

大麻素CB1受体对大鼠视网膜神经节细胞诱发动作电位的作用

蒋淑霞, 李倩, 王霄汉, 李芳, 王中峰*

复旦大学脑科学研究院, 神经生物学研究所, 医学神经生物学国家重点实验室, 上海 200032

摘要: 激活大麻素CB1受体(CB1Rs)通过调控多种离子通道, 从而调节脊椎动物视网膜的功能。本文旨在利用膜片钳全细胞记录技术, 在大鼠视网膜薄片上研究CB1Rs对神经节细胞兴奋性的作用。结果显示, 在电流钳制状态下, 灌流CB1R激动剂WIN55212-2 (WIN, 5 $\mu\text{mol/L}$)对神经节细胞的自发动作电位发放频率和静息膜电位均没有显著影响。在灌流液中加入CNQX, D-APV, bicuculline和strychnine以阻断神经节细胞的兴奋性和抑制性输入, 灌流5 $\mu\text{mol/L}$ WIN对正向电流注入(+10 pA到+100 pA)诱发的动作电位的频率也没有显著影响。位相分析结果显示, 触发动作电位的阈值电位和触发第一个动作电位的延迟时间在加入WIN前后也没有显著改变; 然而, WIN显著降低动作电位的上升和下降相速率($\pm dV/dt_{\text{max}}$), 而且该作用可被CB1R拮抗剂SR141716所阻断。此外, 在阻断突触输入的情况下, WIN对神经节细胞的膜电位也没有显著影响。以上结果提示, 激活大麻素CB1Rs通过调控诱发动作电位, 从而调节大鼠视网膜神经节细胞的兴奋性。

关键词: 动作电位; 大麻素CB1受体; 膜片钳; 神经节细胞; 自发动作电位发放; WIN55212-2

中图分类号: Q424; Q436

Received 2013-03-25 Accepted 2013-05-17

This work was supported by the National Basic Research Development Program of China (No. 2013CB835101), the National Natural Science Foundation of China (No. 30930034), the Key Research Program of Science and Technology Commissions of Shanghai Municipality, China (No. 11JC1401200) and Research Fund for the Doctoral Program of Higher Education of China (No. 20110071110031).

*Corresponding author. Tel: +86-21-54237810; Fax: +86-21-54237643; E-mail: zfwang@fudan.edu.cn

Cannabinoid CB1 receptor (CB1R), a G-protein coupled receptor, which is extensively distributed throughout the central nervous system (CNS) [1–3], plays important roles in regulating multiple neuronal functions, including learning and memory, synaptic plasticity, pain response, and many intracellular signaling pathways [4–8]. Growing evidence has demonstrated that CB1R signaling is also widely expressed in the vertebrate retina [9, 10]. CB1Rs and endocannabinoids (eCBs), including anandamide (AEA) and 2-Arachidonoylglycerol (2-AG), as well as an eCB degradative enzyme, fatty acid amide hydrolase (FAAH), were found in a variety of retinal cell populations and in the inner plexiform layer (IPL) [11–15], suggesting that eCBs may regulate the functions of retinal neurons and participate in multiple circuits of visual information processing. For example, WIN55212-2 (WIN), a CB1R agonist, modulated various types of voltage-gated K^+ and Ca^{2+} currents in retinal photoreceptors and bipolar cells (BCs) [13, 15–17]. Retrograde modulation of glutamate release from cones by 2-AG was found in goldfish [18].

Retinal ganglion cells (RGCs), output neurons of the retina, receive inhibitory inputs from GABAergic and glycinergic amacrine cells (ACs) mediated by $GABA_A$ and glycine receptors and excitatory inputs from BCs mediated by AMPA receptors [19–22]. CB1Rs have been found in BC, ACs and RGCs [11–15]. Activation of CB1Rs in these cells may modulate RGCs excitability, thus influencing visual information processing. However, the effects of CB1R signaling on RGCs are poorly understood. The only evidence was from the cultured RGCs that WIN inhibited Ca^{2+} currents in these cells [11]. In the present work, we studied the effects of WIN on RGC excitability using patch-clamp techniques in rat retinal slices.

1 MATERIALS AND METHODS

All experimental procedures with animals described in the present work were in accordance with the National Institutes of Health (NIH) guidelines for the Care and Use of Laboratory Animals and the guidelines of Fudan University on the ethical use of animals. During this study all efforts were made to minimize the number of animals used and their suffering. Male Sprague-Dawley rats, aged 21–28 d and obtained from SLAC Laboratory Animal Co., Ltd (Shanghai, China), were housed under conditions of a 12 h/12 h light/dark cycle.

1.1 Preparation of retinal slices

The rats were deeply anesthetized with urethane (25 mg/mL) and sacrificed by decapitation. Eyes were enucleated quickly and immersed in ice-cold artificial cerebrospinal fluid (ACSF) containing (in mmol/L): 125 NaCl, 3 KCl, 26 $NaHCO_3$, 1.25 NaH_2PO_4 , 2 $CaCl_2$, 1 $MgCl_2$, 15 glucose (pH 7.4), bubbled with 95% O_2 and 5% CO_2 . Retinae were then isolated and sliced vertically in a thickness of 200 μm on a Narishige slicer (ST-20-P, Tokyo, Japan). Slices were transferred to a holding chamber where they completely submerged in oxygenated ACSF solution and maintained at 33–34 °C for 30 min before recording.

1.2 Electrophysiological recordings

Whole-cell current-clamp recordings were performed using standard techniques [23, 24]. Individual slices were transferred to a perfusing chamber and continuously superfused with oxygenated ACSF at a rate of 1–2 mL/min at 33–34 °C. RGCs in retinal slices were identified by their locations and morphology with the help of an infrared-differential interference contrast (IR-DIC) video microscopy (Olympus, Japan), and further identified by intracellular injection of Lucifer Yellow. Patch pipettes were made by pulling BF150-86-10 glass (Sutter Instrument Co., Novato, CA, USA) on a P-97 Flaming/Brown micropipette puller (Sutter Instrument) and fire polished (Model MF-830, Narishige, Japan) before recording. The pipette resistance was typically 4–8 M Ω after filled with the internal solution (in mmol/L): 120 potassium *D*-gluconate, 1 ethylene glycol-bis(β -aminoethyl ether) N, N, N', N'-tetraacetic acid (EGTA), 10 4-(2-Hydroxyethyl)piperazine-1-ethanesulfonic acid (HEPES), 4 ATP-Mg, 0.3 GTP-Na, 10 phosphocreatine, 0.1 $CaCl_2$, 1 $MgCl_2$, 5 Lucifer Yellow, pH 7.2 adjusted with KOH and to 280–290 mOsm/L. Whole-cell membrane potential were recorded from RGCs by a patch amplifier (Axopatch 700B; Molecular Devices, Foster City, CA, USA) with Digidata 1440A data acquisition board and pClamp 10.2 software at a sampling rate of 10 kHz and a low-pass filter of 1 kHz.

1.3 Drugs and solutions

Bicuculline, *D*-(-)-2-amino-5-phosphonopentanoic acid (D-APV) and 6-Cyano-7-nitroquinoxaline-2,3-dione (CNQX) were purchased from Tocris (Tocris Bioscience, Ellisville, MO, USA) and SR141716 was from Cayman Chemical (Ann Arbor, MI, USA). All others were from Sigma Chemical Company (Sigma-Aldrich, Inc., St. Louis, MO, USA). CNQX, SR141716 and

WIN were first dissolved in dimethyl sulfoxide (DMSO) and then diluted in ACSF solution with a final DMSO concentration less than 0.1%, which has no significant effects on membrane response of RGCs. All other chemicals were prepared in distilled water, stored at -20°C and freshly diluted to the final concentration using ACSF solution.

1.4 Data analysis

Data analysis was performed off-line using the Clampfit 10.2 (Molecular Devices, Foster City, CA, USA) and MATLAB R2011a (MathWorks, USA). For action potential analysis, the temporal derivative dV/dt was first calculated by the equation of the form $dV/dt(t_n) = (V_{n+1} - V_{n-1}) / 2\Delta t$, and then plotted it against the instantaneous membrane potential to yield the phase-plane plot [25, 26]. The threshold voltage for triggering the first action potential was determined using a criterion that the velocity of action potential reaching 20 mV/ms. Data are presented as mean \pm SEM. Paired t test was used for statistical analysis, and a P value < 0.05 was considered statistically significant.

2 RESULTS

2.1 WIN does not change spontaneous firing and membrane potential of RGCs

RGCs display spontaneous firing under physiological condition [27]. We first examined whether activation of CB1Rs may affect spontaneous firing of rat RGCs. As shown in Fig. 1A, perfusion of WIN (5 $\mu\text{mol/L}$) for 10 min did not change the spontaneous firing frequency in a RGC (upper trace). The average firing frequency (from 9 to 10 min after WIN application) obtained from 10 cells was (0.88 ± 0.49) Hz, which was not significantly different from that before WIN application ($0.40 \text{ Hz} \pm 0.17 \text{ Hz}$) ($P = 0.125$, Fig. 1B). At the same time, WIN also hardly changed resting membrane potential of the cell (Fig. 1A, lower enlarged trace), with the average being (-56.48 ± 1.09) mV ($n = 10$, $P = 0.356$ vs control value of $-56.08 \text{ mV} \pm 1.23 \text{ mV}$) (Fig. 1C).

2.2 Effects of WIN on evoked action potentials of rat RGCs

In order to test whether WIN may directly influence intrinsic excitability of rat RGC, we perfused cocktail synaptic blockers, including bicuculline (10 $\mu\text{mol/L}$), strychnine (10 $\mu\text{mol/L}$), CNQX (10 $\mu\text{mol/L}$) and D-APV (50 $\mu\text{mol/L}$), to obstruct the synaptic inputs, and then examined the effects of WIN on RGCs. Fig. 2A

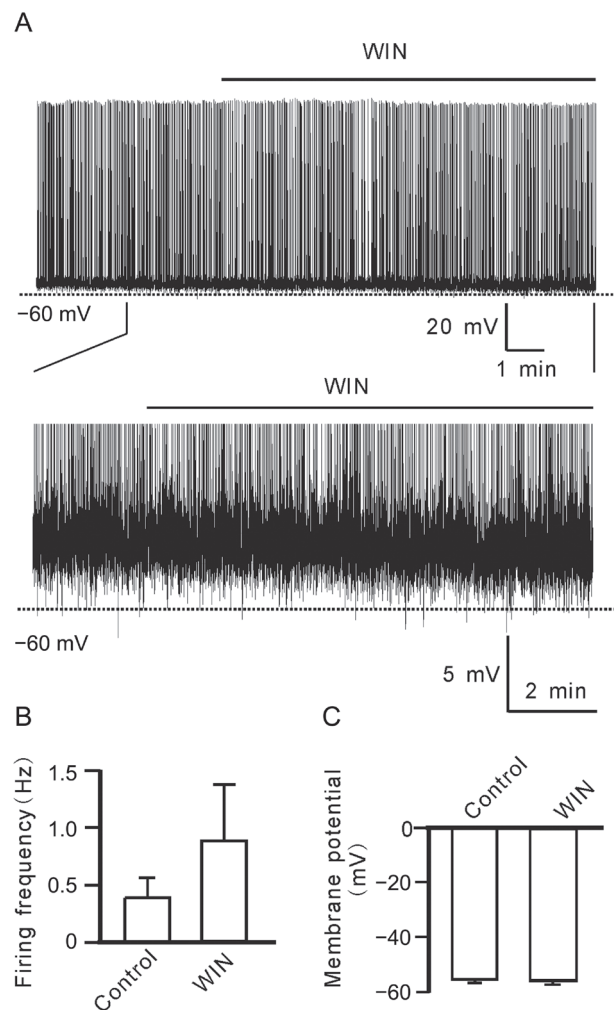


Fig. 1. WIN55212-2 (WIN) does not affect spontaneous firing and resting membrane potential of RGCs in retinal slices with synaptic inputs being intact. *A*: Representative trace recorded from a RGC, showing that extracellular application of WIN (5 $\mu\text{mol/L}$) did not affect spontaneous firing and resting membrane potential of the cell. Lower trace is enlarged one to show change of membrane potential. *B*, *C*: Bar charts summarizing the changes of spontaneous firing frequency (*B*) and membrane potential (*C*) of RGCs before and after application of WIN. Data are presented as mean \pm SEM, $n = 10$.

and 2B show membrane responses of a RGC to a series of 500 ms positive injected currents from +10 pA to +100 pA in a 10 pA increment before and 10 min after perfusing 5 $\mu\text{mol/L}$ WIN. The range of injected currents was enough to induce appropriate firing in RGCs. WIN did not remarkably change firing pattern and frequency of the cell. Fig. 2C shows representative recordings in a +20 pA current injection. Data analysis revealed that the firing frequency of the cells was in-

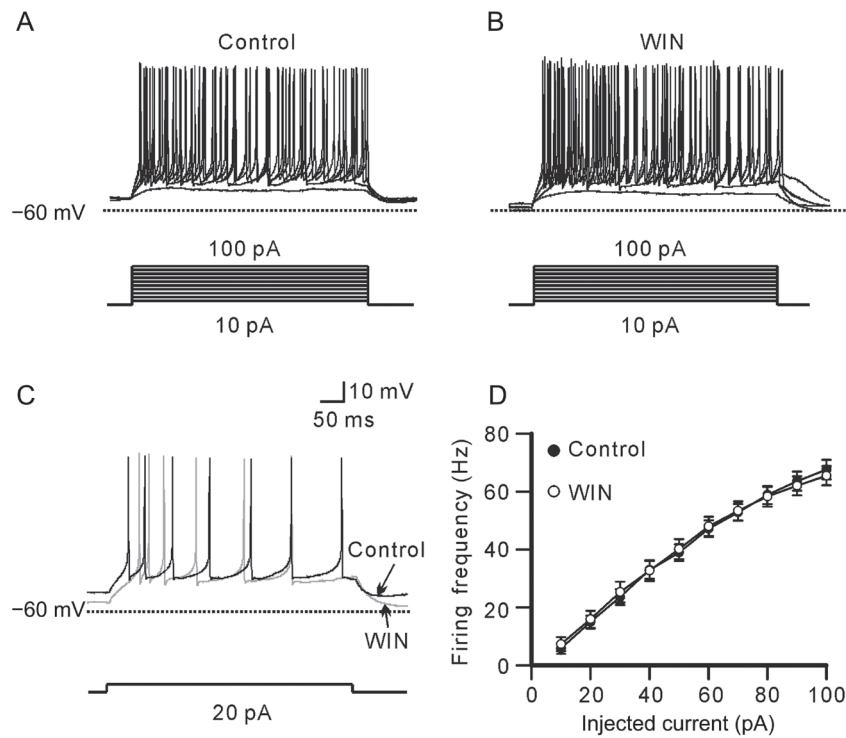


Fig. 2. WIN does not affect firing frequency of evoked action potentials of RGCs with synaptic inputs being blocked. *A, B*: Representative traces obtained from a RGC, showing the effect of WIN (5 $\mu\text{mol/L}$) on firing frequency of evoked action potentials before (*A*) and after application of 5 $\mu\text{mol/L}$ WIN (*B*). A series of positive currents ranging from +10 pA to +100 pA was injected. *C*: Sample traces show that 5 $\mu\text{mol/L}$ WIN did not significantly affect firing frequency of action potentials evoked by +20 pA current injection in a RGC. *D*: Plot of average firing frequency of evoked action potentials versus different injected currents, showing that WIN did not change firing frequency of the action potentials at all injected current levels. Data are presented as mean \pm SEM, $n = 17$.

creased accompanying with increased positive current injection (Fig. 2D). The average firing frequency was increased from (5.76 ± 1.85) Hz to (67.60 ± 3.33) Hz ($n = 17$) when the injected current was from +10 pA to +100 pA in control, while it was from (7.29 ± 2.45) Hz to (65.47 ± 3.33) Hz ($n = 17$) after WIN application. There was no significant difference before and after WIN application at all injected current levels (Fig. 2D).

We analyzed the effects of WIN on individual action potential evoked by current injection. For simple purpose, we only chose and analyzed the first action potential in each current injection [25, 26]. Fig. 3A shows representative phase-plane trajectories of the action potentials before (control) and after WIN application. Fig. 3B is an enlarged figure from the square as shown in Fig. 3A, clearly showing unchanged threshold voltages. The average threshold voltage for triggering action potential was from (-41.04 ± 2.14) mV to (-43.15 ± 2.04) mV as injected currents were increased from +10 pA to +100 pA after WIN application, which were not significantly different from those of control (from

$-41.49 \text{ mV} \pm 2.10 \text{ mV}$ to $-43.93 \text{ mV} \pm 2.14 \text{ mV}$, $n = 17$) (Fig. 3C). Moreover, the delay time from onset of current injection to the threshold voltage for triggering the first action potential was also unchanged after WIN application, with the average being from $169.3 \text{ ms} \pm 17.6 \text{ ms}$ to $102.3 \text{ ms} \pm 0.9 \text{ ms}$ ($n = 17$) at +10 pA to +100 pA current injection respectively, comparable to the control levels ($178.8 \text{ ms} \pm 11.7 \text{ ms}$ to $102.9 \text{ ms} \pm 0.8 \text{ ms}$, $n = 17$) (Fig. 3D).

Although WIN did not influence the threshold voltage for triggering action potential and the delay time to reach threshold voltage, it is clearly shown from phase-plane plots of the action potentials that WIN may change the rate of both depolarizing and repolarizing phases (Fig. 3A). Pooled data from 17 cells revealed that WIN may somewhat modulate maximum rising phase rate ($+dV/dt_{\text{max}}$) of the action potentials (Fig. 3E). Specifically, the $+dV/dt_{\text{max}}$ (mV/ms) was significantly reduced at +20 pA (179.7 ± 12.3 vs 189.1 ± 13.7 , $P = 0.049$), +30 pA (179.1 ± 10.5 vs 187.5 ± 12.8 , $P = 0.043$), +50 pA (183.8 ± 11.2 vs 193.3 ± 12.7 , $P =$

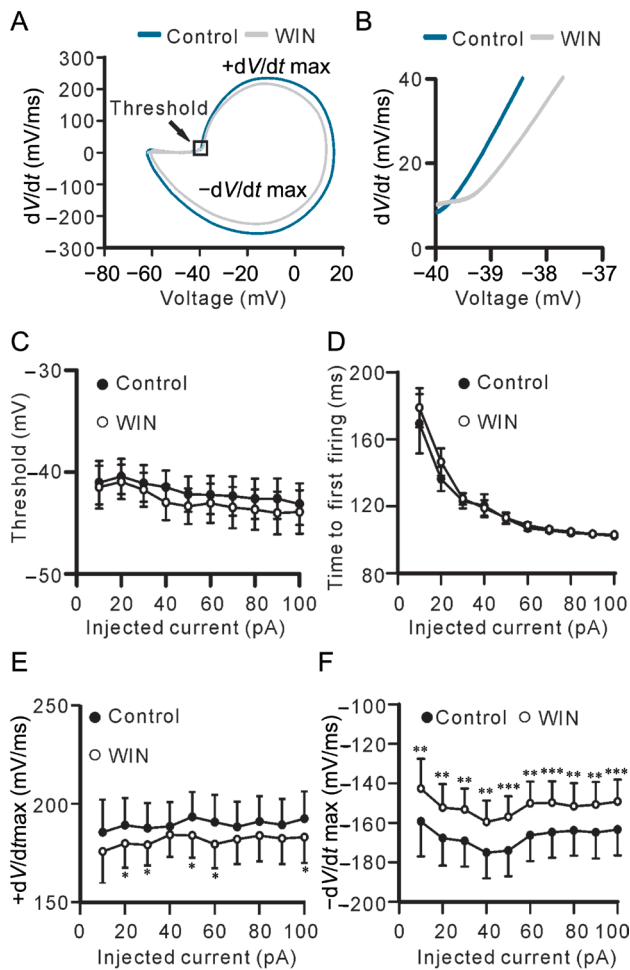


Fig. 3. WIN reduces rising and descending phase velocities of evoked action potential of RGCs. *A*: Representative phase-plane plots of action potentials before (control) and after 5 $\mu\text{mol/L}$ WIN application. *B*: Enlarged figure obtained from the square in *A*, showing that WIN did not change threshold voltage for triggering the first action potential of a RGC. *C*: Plots of average threshold voltage for triggering the first action potential versus different injected currents, showing that WIN did not change the threshold voltage at all injected current levels. *D*: Plots of average time from onset of current injection to first action potential versus different injected currents, showing that WIN did not change the delay time at all injected current levels. *E*, *F*: Plots of average $+dV/dt_{\text{max}}$ and $-dV/dt_{\text{max}}$ of action potentials versus different injected currents, showing that WIN reduced $+dV/dt_{\text{max}}$ of action potentials at some injected current levels, and $-dV/dt_{\text{max}}$ of action potentials at all injected current levels. Data are presented as mean \pm SEM, $n = 17$. * $P < 0.05$, ** $P < 0.01$ and *** $P < 0.001$ vs control.

0.046), +60 pA (179.4 ± 12.2 vs 190.7 ± 13.8 , $P = 0.020$) and +100 pA current injection (183.0 ± 13.1 vs 192.4 ± 13.8 , $P = 0.026$), respectively. Meanwhile,

Table 1. Changes of maximum rising phase rate ($+dV/dt_{\text{max}}$, mV/ms) of the action potentials in control and in the presence of SR141716 and WIN55212-2

Injected current (pA)	Control	SR141716+ WIN55212-2	<i>P</i> value
10	210.2 ± 25.1	193.3 ± 33.6	0.297
20	187.4 ± 12.8	186.2 ± 15.7	0.791
30	187.3 ± 15.5	179.5 ± 14.5	0.364
40	183.5 ± 14.4	183.6 ± 15.3	0.990
50	185.5 ± 15.7	180.5 ± 16.9	0.513
60	182.7 ± 14.4	179.0 ± 15.5	0.431
70	186.1 ± 16.9	183.6 ± 17.6	0.754
80	185.6 ± 16.3	182.1 ± 18.4	0.669
90	185.7 ± 17.7	180.4 ± 15.3	0.502
100	180.4 ± 15.0	178.3 ± 16.3	0.786

Data are presented as mean \pm SEM, $n = 5$.

Table 2. Changes of maximum descending phase rate ($-dV/dt_{\text{max}}$, mV/ms) of the action potentials in control and in the presence of SR141716 and WIN55212-2

Injected current (pA)	Control	SR141716 +WIN55212-2	<i>P</i> value
10	-176.1 ± 59.4	-161.1 ± 59.1	0.604
20	-159.6 ± 20.8	-154.6 ± 22.5	0.243
30	-159.1 ± 20.6	-152.9 ± 20.9	0.237
40	-156.7 ± 20.4	-150.7 ± 19.7	0.320
50	-154.2 ± 18.9	-152.6 ± 21.5	0.754
60	-153.9 ± 19.5	-148.9 ± 19.1	0.462
70	-159.1 ± 20.5	-152.3 ± 21.4	0.229
80	-155.2 ± 19.5	-152.3 ± 21.7	0.621
90	-156.1 ± 19.9	-149.1 ± 22.1	0.176
100	-154.8 ± 20.3	-148.7 ± 20.2	0.299

Data are presented as mean \pm SEM, $n = 5$.

WIN remarkably reduced maximum descending phase rate ($-dV/dt_{\text{max}}$) of the action potentials at all current injected levels ($n = 17$, P all < 0.01 or 0.001) (Fig. 3*F*). In addition, WIN-induced effects on $\pm dV/dt_{\text{max}}$ of evoked action potentials were eliminated by co-application of SR141716 (300 nmol/L), a CB1R antagonist. As shown in Table 1 and Table 2, co-applying SR141716 and WIN for 10 min, $\pm dV/dt_{\text{max}}$ of action potentials at all current injected levels were comparable to control.

2.3 WIN does not change resting membrane potential of RGCs in the absence of synaptic inputs

Finally, we tested the effects of WIN on resting membrane potential of RGCs in the absence of synaptic inputs. As shown in Fig. 4*A*, after spontaneous firing

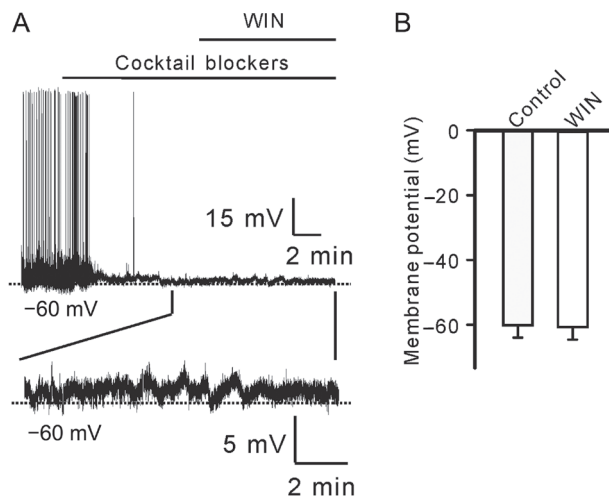


Fig. 4. WIN does not change resting membrane potentials of RGCs with synaptic inputs being blocked. *A*: Representative trace shows the effect of WIN on resting membrane potential of a RGC. Lower trace is enhanced one to show change of membrane potential. Note that WIN did not induce changes of membrane potential of the cell. *B*: Bar chart summarizing the changes of resting membrane potential of RGCs before and after application of WIN. Data are presented as mean \pm SEM, $n = 5$.

was blocked by perfusing cocktail synaptic blockers, WIN (5 μ mol/L) was applied to a RGC in retinal slice. WIN failed to induce the cell to firing. Enlarged figure clearly shows that membrane potential of the cell was not significantly changed 10 min after WIN application. Summary data obtained from 5 cells revealed that the average resting potential was (-61.3 ± 3.9) mV in the presence of WIN, comparable to that of control $(-60.8 \text{ mV} \pm 3.9 \text{ mV}, n = 5, P = 0.138)$ (Fig. 4B).

3 DISCUSSION

In the inner retina, BCs, ACs and RGCs form a neuronal circuit that transmits the visual signals and modulates the visual information processing. The excitability of RGCs is determined by the balance of inhibitory and excitatory inputs, as well as the intrinsic properties of the cells. The present results showed that cannabinoid receptor agonist WIN did not significantly change spontaneous firing frequency of rat RGCs with synaptic inputs being intact (Fig. 1), suggesting that WIN may not influence intrinsic electrophysiological properties of RGCs under such condition. This was supported by the fact that WIN had no significant effect on resting membrane potential of RGCs without synaptic inputs being blocked by cocktail synaptic blockers (Fig. 1).

Considering that RGCs receive both inhibitory and excitatory inputs from ACs and BCs [19–22], and activation of CB1Rs at the terminals of ACs and BCs by WIN inhibited spontaneous release of GABA and glutamate [28], WIN may simultaneously modulate inhibitory and excitatory inputs of RGCs, thus not disturbing the balance of inhibitory and excitatory inputs of the cells.

Although WIN did not affect resting membrane potential of rat RGCs, it remarkably reduced rising and descending rates of evoked action potentials (Fig. 3). Previous studies have shown that WIN concentration dependently inhibited voltage-gated sodium currents (I_{Na}) in cultured rat trigeminal ganglion cells via CB1Rs [29]. AEA also inhibited I_{Na} in rat dorsal root ganglion neurons, and the effect was not reversed by AM251 and AM630, suggestive of a direct action of AEA on Na^+ channels [30]. Na^+ channels were expressed in rat RGCs and involved in the generation of rising phase of action potential [29]. WIN-induced reduction of $+dV/dt_{\text{max}}$ of action potential may be due to its inhibitory effect on Na^+ channels. Moreover, cannabinoid-induced suppression of Ca^{2+} channels may also partially contribute to WIN-induced reduction of $+dV/dt_{\text{max}}$ of action potential [11]. Descending phase of action potential is contributed by K^+ channels [31, 32]. RGCs expressed multiple types of voltage-gated K^+ channels [25, 33–36], and activation of cannabinoid receptors by WIN may modulate various K^+ currents in photoreceptors and BCs [13, 15–17]. WIN-induced reduction of $-dV/dt_{\text{max}}$ of action potential may be resulted from its inhibition on K^+ channels. Furthermore, WIN-induced effect on action potential was mediated by CB1Rs because SR141716 could reverse WIN effect. On the other hand, WIN did not change the resting membrane potential and spontaneous firing of RGCs with or without synaptic inputs being blocked by cocktail synaptic blockers, suggesting that WIN had no modulating roles on the K^+ channels, such as inward rectifying (Kir) and small-conductance Ca^{2+} -activated K^+ (SK_{Ca}) channels, as well as hyperpolarization-activated cation channels (I_{h}), which are involved in the generation of resting membrane potential and after-hyperpolarization potential.

The present work demonstrated that activation of CB1Rs regulates rat RGC excitability through modulating rising and descending rates of evoked action potentials of the cells.

REFERENCES

- 1 Hashimoto-dani Y, Ohno-Shosaku T, Kano M. Endocannabi-

- noids and synaptic function in the CNS. *Neuroscientist* 2007; 13: 127–137.
- 2 Herkenham M, Lynn AB, Little MD, Johnson MR, Melvin LS, de Costa BR, Rice KC. Cannabinoid receptor localization in brain. *Proc Nat Acad Sci U S A* 1990; 87: 1932–1936.
 - 3 Matsuda LA, Lolait SJ, Brownstein MJ, Young AC, Bonner TI. Structure of a cannabinoid receptor and functional expression of the cloned cDNA. *Nature* 1990; 346: 561–564.
 - 4 Chevaleyre V, Takahashi KA, Castillo PE. Endocannabinoid-mediated synaptic plasticity in the CNS. *Annu Rev Neurosci* 2006; 29: 37–76.
 - 5 Galve-Poperh I, Aguado T, Palazuelos J, Guzman M. The endocannabinoid system and neurogenesis in health and disease. *Neuroscientist* 2007; 13: 109–114.
 - 6 Kreitzer AC, Regehr WG. Retrograde inhibition of presynaptic calcium influx by endogenous cannabinoids at excitatory synapses onto Purkinje cells. *Neuron* 2001; 29: 717–727.
 - 7 Ohno-Shosaku T, Maejima T, Kano M. Endogenous cannabinoids mediate retrograde signals from depolarized postsynaptic neurons to presynaptic terminals. *Neuron* 2001; 29: 729–738.
 - 8 Wilson RI, Nicoll RA. Endogenous cannabinoids mediate retrograde signalling at hippocampal synapses. *Nature* 2001; 410: 588–592.
 - 9 Yazulla S. Endocannabinoids in the retina: from marijuana to neuroprotection. *Prog Retin Eye Res* 2008; 27: 501–526.
 - 10 Zabouri N, Bouchard JF, Casanova C. Cannabinoid receptor type 1 expression during postnatal development of the rat retina. *J Comp Neurol* 2011; 519: 1258–1280.
 - 11 Lalonde MR, Jollimore CA, Stevens K, Barnes S, Kelly ME. Cannabinoid receptor-mediated inhibition of calcium signaling in rat retinal ganglion cells. *Mol Vis* 2006; 12: 1160–1166.
 - 12 Porcella A, Maxia C, Gessa GL, Pani L. The human eye expresses high levels of CB1 cannabinoid receptor mRNA and protein. *Eur J Neurosci* 2000; 12: 1123–1127.
 - 13 Straiker AJ, Maguire G, Mackie K, Lindsey J. Localization of cannabinoid CB1 receptors in the human anterior eye and retina. *Invest Ophthalmol Vis Sci* 1999; 40: 2442–2448.
 - 14 Yazulla S, Studholme KM, McIntosh HH, Deutsch DC. Immunocytochemical localization of cannabinoid CB1 receptor and fatty acid amide hydrolase in rat retina. *J Comp Neurol* 1999; 415: 80–90.
 - 15 Yazulla S, Studholme KM, McIntosh HH, Fan SF. Cannabinoid receptors on goldfish retinal bipolar cells: electron-microscope immunocytochemistry and whole-cell recordings. *Vis Neurosci* 2000; 17: 391–401.
 - 16 Fan SF, Yazulla S. Biphasic modulation of voltage-dependent currents of retinal cones by cannabinoid CB1 receptor agonist WIN 55212–2. *Vis Neurosci* 2003; 20: 177–188.
 - 17 Straiker A, Sullivan JM. Cannabinoid receptor activation differentially modulates ion channels in photoreceptors of the tiger salamander. *J Neurophysiol* 2003; 89: 2647–2654.
 - 18 Fan SF, Yazulla S. Retrograde endocannabinoid inhibition of goldfish retinal cones is mediated by 2-arachidonoyl glycerol. *Vis Neurosci* 2007; 24: 257–267.
 - 19 Marc RE, Liu W. Fundamental GABAergic amacrine cell circuitries in the retina: nested feedback, concatenated inhibition, and axosomatic synapses. *J Comp Neurol* 2000; 425: 560–582.
 - 20 Protti DA, Gerschenfeld HM, Llano I. GABAergic and glycinergic IPSCs in ganglion cells of rat retinal slices. *J Neurosci* 1997; 17: 6075–6085.
 - 21 Wässle H. Parallel processing in the mammalian retina. *Nat Rev Neurosci* 2004; 5: 747–757.
 - 22 Wässle H, Boycott BB. Functional architecture of the mammalian retina. *Physiol Rev* 1991; 71: 447–480.
 - 23 Yang XF, Miao Y, Ping Y, Wu HJ, Yang XL, Wang Z. Melatonin inhibits tetraethylammonium-sensitive potassium channels of rod ON type bipolar cells via MT₂ receptors in rat retina. *Neuroscience* 2011; 173: 19–29.
 - 24 Zhao WJ, Zhang M, Miao Y, Yang XL, Wang Z. Melatonin potentiates glycine currents through a PLC/PKC signaling pathway in rat retinal ganglion cells. *J Physiol (Lond)* 2010; 588: 2605–2619.
 - 25 Fohlmeister JF, Cohen ED, Newman EA. Mechanisms and distribution of ion channels in retinal ganglion cells: using temperature as an independent variable. *J Neurophysiol* 2010; 103: 1357–1374.
 - 26 Naundorf B, Wolf F, Volgushev M. Unique features of action potential initiation in cortical neurons. *Nature* 2006; 440: 1060–1063.
 - 27 Margolis DJ, Detwiler PB. Different mechanisms generate maintained activity in ON and OFF retinal ganglion cells. *J Neurosci* 2007; 27: 5994–6005.
 - 28 Middleton TP, Protti DA. Cannabinoids modulate spontaneous synaptic activity in retinal ganglion cells. *Vis Neurosci* 2011; 28: 393–402.
 - 29 Fu H, Xiao JM, Cao XH, Ming ZY, Liu LJ. Effects of WIN55,212-2 on voltage-gated sodium channels in trigeminal ganglion neurons of rats. *Neurosci Res* 2008; 30: 85–91.
 - 30 Kim HI, Kim TH, Shin YK, Lee CS, Park M, Song JH. Anandamide suppression of Na⁺ currents in rat dorsal root ganglion neurons. *Brain Res* 2005; 1062: 39–47.
 - 31 Jensen RJ, DeVoe RD. Comparisons of directionally selective with other ganglion cells of the turtle retina: intracellular recording and staining. *J Comp Neurol* 1983; 217: 271–287.
 - 32 Karschin A, Lipton SA. Calcium channels in solitary retinal ganglion cells from post-natal rat. *J Physiol (Lond)* 1989;

- 418: 379–396.
- 33 Clark BD, Kurth-Nelson ZL, Newman EA. Adenosine-evoked hyperpolarization of retinal ganglion cells is mediated by G-protein-coupled inwardly rectifying K⁺ and small conductance Ca²⁺-activated K⁺ channel activation. *J Neurosci* 2009; 29: 11237–11245.
- 34 Ettaiche M, Heurteaux C, Blondeau N, Borsotto M, Tinel N, Lazdunski M. ATP-sensitive potassium channels K_{ATP} in retina: a key role for delayed ischemic tolerance. *Brain Res* 2001; 890: 118–129.
- 35 Koeberle PD, Wang Y, Schlichter LC. Kv1.1 and Kv1.3 channels contribute to the degeneration of retinal ganglion cells after optic nerve transection *in vivo*. *Cell Death Differ* 2010; 17: 134–144.
- 36 Lipton SA, Tauck DL. Voltage-dependent conductances of solitary ganglion cells dissociated from the rat retina. *J Physiol (Lond)* 1987; 385: 361–391.